

# THE CANADIAN MINERALOGIST

*Canadian Mineralogist*  
Vol. 30, pp. 1-18 (1992)

## A COMPREHENSIVE STRUCTURE-MODEL FOR VESUVIANITE: SYMMETRY VARIATIONS AND CRYSTAL GROWTH

FRED M. ALLEN\* AND CHARLES W. BURNHAM

*Department of Earth and Planetary Sciences, Harvard University, Cambridge, Massachusetts 02138, U.S.A.*

### ABSTRACT

We have developed a comprehensive model of the vesuvianite structure that accounts for: (1) the diversity of observed space-groups, (2) anomalous optical properties, and (3) the deviation in chemical composition from proposed formulae. The model proposes variation in the degree of cation-vacancy ordering on the partially filled *B* and *C* sites, as well as positional ordering of ions surrounding *B* and *C*. The *B* and *C* positions are constrained to be occupied in an alternating manner, indicating short-range order at the unit-cell level. Differently ordered unit-cells are related by merohedral, or nearly merohedral, twinning. Two structural forms of vesuvianite are distinguished on the basis of the size of ordered domains. High-symmetry vesuvianite has a long-range disordered structure with  $P4/nnc$  average symmetry. Low-symmetry vesuvianite contains ordered domains based on  $P4/n$ ,  $P\bar{4}$ ,  $P4nc$ , or lower symmetry. Crystals containing equal volumes of oppositely ordered domains exhibit  $P4/nnc$  pseudosymmetry (long-range disorder); those with unequal volumes exhibit bulk symmetry consistent with the preferred scheme of order (partial long-range order). Low vesuvianite occurs in metamorphic rocks formed at low temperatures (<300°C) compared to those containing high vesuvianite (400–800°C). Ordering in low vesuvianite presumably takes place during crystal growth rather than by an ordering transformation on cooling.

*Keywords:* vesuvianite, crystal structure, order/disorder, crystal growth, domain structures, symmetry.

### SOMMAIRE

Nous présentons un modèle général de la structure de la vésuvianite qui rend compte (1) de la diversité des groupes spatiaux observés, (2) des propriétés optiques anormales, et (3) des écarts à la formule idéale. Le modèle propose des variations dans le degré d'ordre impliquant cations et lacunes dans les sites *B* et *C*, partiellement occupés, de même qu'un désordre de position des ions qui jouxtent ces deux sites. Les positions *B* et *C* doivent être remplies en alternance, indication d'un degré d'ordre à l'échelle des mailles élémentaires. Des mailles ayant des degrés d'ordre différents obéissent à une relation de maclé méroédrique (ou presque). Deux formes structurales de vésuvianite se distinguent par la dimension des domaines ordonnés. La vésuvianite dite de symétrie élevée possède une structure désordonnée à longue échelle, et une symétrie moyenne  $P4/nnc$ . La vésuvianite dite de symétrie inférieure contient des domaines ordonnés et possède une symétrie  $P4/n$ ,  $P\bar{4}$ ,  $P4nc$ , ou une symétrie inférieure. Les cristaux qui contiennent des volumes égaux de domaines mis en ordre de façon opposée font preuve d'une pseudo-symétrie  $P4/nnc$  (désordre à longue échelle). Ceux dont les domaines occupent des volumes inégaux possèdent une symétrie d'ensemble qui concorde avec le schéma de mise en ordre prédominant (ordre partiel à longue échelle). La vésuvianite de symétrie inférieure est typique de roches métamorphiques formées à de faibles températures (<300°C), tandis que la vésuvianite de symétrie élevée se serait formée à une température plus

\*Present address: Engelhard Corporation, Research and Development, 101 Wood Avenue, Iselin, New Jersey 08830, U.S.A.

élevée (400–800°C). La mise en ordre nécessaire pour atteindre la vésuvianite de symétrie inférieure accompagne la croissance des cristaux plutôt que d'apparaître progressivement par transformation ultérieure, pendant le refroidissement.

(Traduit par la Rédaction)

**Mots-clés:** vésuvianite, structure cristalline, relation ordre-désordre, croissance cristalline, structure en domaines, symétrie.

## INTRODUCTION

The  $P4/nnc$  structure model of vesuvianite, first proposed by Warren & Modell (1931) and later modified by Coda *et al.* (1970) and Rucklidge *et al.* (1975), is built up of fragments of the grossular structure alternating with regions containing unusual partly filled cation-polyhedra (Fig. 1). The model, although fundamentally correct, fails to account fully for observed variations in the symmetry of vesuvianite. Some symmetry variations had been recognized before the vesuvianite structure had actually been solved by Warren & Modell. Mineralogists of the late 1800s and early 1900s described the "anomalous" optical properties of vesuvianite from various localities [see Arem (1973) and Deer *et al.* (1982) for reviews]. Reports had been made of sector-zoned crystals that exhibit both uniaxial and biaxial characteristics. Arem & Burnham (1969) reported that violations of  $P4/nnc$

glide-plane extinction criteria appear on single-crystal X-ray photographs of vesuvianite from some localities. Coda *et al.* (1970) then suggested that ordering of atoms occupying partly filled sites along the 4-fold axes (the *B* and *C* sites) would lower the symmetry and thus explain these observations. The existence of incompletely ordered vesuvianite was confirmed by Giuseppetti & Mazzi (1983) and Allen & Burnham (1983b). Fitzgerald *et al.* (1986b, 1987) refined structures of low-symmetry vesuvianite in space group  $P4/n$ . Allen (1985) carried out a refinement in space group  $P4$ .

According to these authors, different structural forms of vesuvianite can be distinguished on the basis of the size of ordered domains, defined as groups of unit cells whose symmetry can be resolved. A perfect domain consists of identically ordered unit cells; an imperfect domain consists of unit cells based on a predominant scheme of order. Diffraction maxima that violate glide-plane extinction criteria appear if the structure consists of domains based on  $P4/n$ ,  $P4nc$ , or lower symmetry. The larger the domains, the more intense are the glide-violating diffractions (GVDs). A positive piezoelectric test presumably results if domains obey acentric subgroup symmetry of  $P4/nnc$ , such as, for example,  $P4nc$ . As the size of the domains decreases, the intensities of the GVDs decrease, and the structure becomes that of disordered vesuvianite with  $P4/nnc$  symmetry.

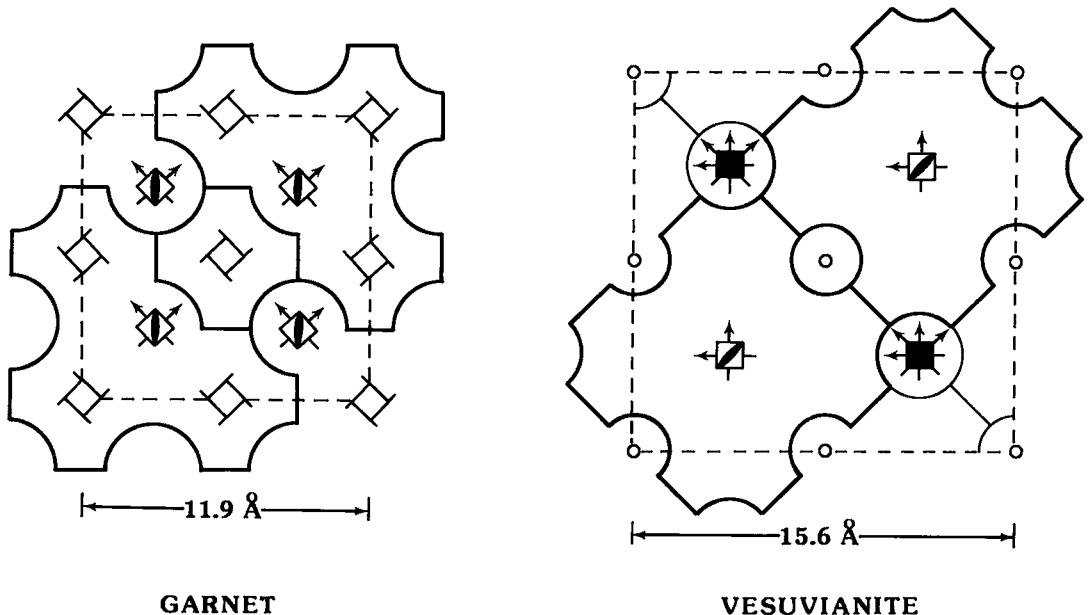


FIG. 1. Schematic representation of the relation between the structure of grossular garnet ( $Ia3d$ ) and vesuvianite ( $P4/nnc$ ). The atomic arrangement within the four-sided figures is identical in the two structures.

Allen (1985) and Allen & Burnham (1985) have reported a connection between the symmetry of vesuvianite and its mode of occurrence or environment of crystal growth. The purpose of this paper is to elaborate on the distinction between "high-symmetry" and "low-symmetry" vesuvianite, and to discuss the geological origin of these different forms.

### EXPERIMENTAL

Vesuvianite specimens from about twenty localities have been examined using a variety of techniques. Most of the specimens were obtained from the research collection at the Harvard Mineralogical Museum. Allen (1985) gave detailed experimental procedures and sample descriptions; only an overview is provided here.

Thin sections prepared in (001) and (100) orientations were examined to detect non-uniaxial optical behavior, twinning, and sector-growth phenomena. Single crystals suitable for study by X-ray diffraction were extracted from thin sections wherever possible; otherwise they were obtained from samples that had been granulated and sieved.

GVDs were detected on precession and Weissenberg single-crystal X-ray-diffraction photographs. Precision back-reflection Weissenberg photographs were measured to provide high-precision cell

dimensions for high vesuvianite from Luning, Nevada and low vesuvianite from Eden Mills, Vermont. Powder X-ray-diffraction data for several samples were recorded using both conventional and synchrotron sources, but these failed to differentiate high from low vesuvianite. To investigate the variation of intensities of GVDs with temperature, *in situ* heating experiments were conducted with an automated single-crystal diffractometer; precession photographs of samples that had been heated and then quenched were examined.

Structure refinements with single-crystal X-ray intensity data were completed on samples from six localities, as summarized in Table 1. Detailed results of these refinements have been given by Allen (1985). Second harmonic generation (SHG) was employed as a test for acentricity to help constrain the choice of space group. The SHG technique is described by Dougherty & Kurtz (1976).

Both powders and ion-milled thin sections of several samples of vesuvianite were examined with transmission electron microscopy. Selected-area electron diffraction (SAED) was used to compare the diffuseness of GVDs in samples from several different localities; diffuseness is used as an indication of the presence of fine-scale short-range-ordered domains. Veblen & Wiechmann (1991) discussed streaking in vesuvianite SAED patterns

TABLE 1. PHYSICAL AND CHEMICAL DATA AND STRUCTURE REFINEMENT RESULTS FOR VESUVIANITE SAMPLES EXAMINED IN THIS STUDY

| Specimen locality | Cell parameters (Å) <sup>1</sup> |                |            | Refinement results <sup>2</sup> |      |                |       |
|-------------------|----------------------------------|----------------|------------|---------------------------------|------|----------------|-------|
|                   | a <sub>1</sub>                   | a <sub>2</sub> | c          | Sp. Gp.                         | R    | R <sub>w</sub> | # UDs |
| High vesuvianite  |                                  |                |            |                                 |      |                |       |
| 1 Luning, NV      | 15.559(4)                        | 15.567(4)      | 11.819(2)  | <i>P4/nnc</i>                   | .046 | .044           | 3830  |
| 2 Sanford, ME     |                                  | 15.5333(2)     | 11.7778(2) | <i>P4/nnc</i>                   | .048 | .040           | 3094  |
| 3 Franklin, NJ    | 15.535(3)                        | 15.535(3)      | 11.790(1)  | <i>P4/nnc</i>                   | .056 | .058           | 3189  |
| Low vesuvianite   |                                  |                |            |                                 |      |                |       |
| 4 Asbestos, QC    | 15.532(2)                        | 15.535(2)      | 11.812(2)  | <i>P4/nnc</i>                   | .086 | .070           | 2525  |
| 5 Georgetown, CA  | 15.520(3)                        | 15.521(3)      | 11.818(2)  | <i>P4/nnc</i>                   | .064 | .063           | 3502  |
| 6 Eden Mills, VT  | 15.554(3)                        | 15.565(4)      | 11.831(3)  | <i>P4̄</i>                      | .061 | .033           | 3819  |

<sup>1</sup> Cell parameters refined from 20 or more single-crystal X-ray diffractions. Values for Sanford vesuvianite are high-precision cell parameters from Arem (1970). Standard deviations in parentheses.

<sup>2</sup> X-ray structure refinement results include space group (Sp. Gp.), unweighted residual (R), weighted residual (R<sub>w</sub>), and number of unrejected diffractions (# UDs). Anisotropic temperature-factors used in all refinements except Eden Mills *P4̄*, to which isotropic temperature-factors were applied.

Chemical formulae and colors of crystals:

- Ca<sub>18.8</sub>(Al<sub>10.3</sub>Mg<sub>2.6</sub>Fe<sup>3+</sup><sub>0.3</sub>)(Al<sub>0.4</sub>Si<sub>17.6</sub>)(O<sub>68.3</sub>OH<sub>9.3</sub>F<sub>0.4</sub>); pale green
- (Ca<sub>18.6</sub>Na<sub>0.1</sub>)(Al<sub>10.0</sub>Mg<sub>1.1</sub>Tl<sub>0.2</sub>Mn<sub>0.2</sub>Fe<sup>3+</sup><sub>0.3</sub>Fe<sup>2+</sup><sub>1.3</sub>)(Al<sub>0.2</sub>Si<sub>17.8</sub>)(O<sub>68.6</sub>OH<sub>6.2</sub>F<sub>3.2</sub>); brown
- (Ca<sub>18.5</sub>Na<sub>0.4</sub>)(Al<sub>10.3</sub>Mg<sub>0.2</sub>Mn<sub>0.4</sub>Fe<sup>3+</sup><sub>0.8</sub>Cu<sub>0.5</sub>Zn<sub>0.9</sub>)(Al<sub>0.1</sub>Si<sub>17.9</sub>)(O<sub>68.8</sub>OH<sub>7.6</sub>F<sub>1.8</sub>); blue
- Ca<sub>18.9</sub>(Al<sub>11.1</sub>Mg<sub>1.9</sub>Fe<sup>3+</sup><sub>0.1</sub>)Si<sub>18.0</sub>(O<sub>69.2</sub>OH<sub>8.6</sub>F<sub>0.2</sub>); colorless
- Ca<sub>19.0</sub>(Al<sub>10.8</sub>Mg<sub>1.8</sub>Fe<sup>3+</sup><sub>0.4</sub>)(Al<sub>0.1</sub>Si<sub>17.9</sub>)(O<sub>69.1</sub>OH<sub>8.7</sub>F<sub>0.2</sub>); pale yellow
- Ca<sub>19.0</sub>(Al<sub>9.4</sub>Mg<sub>1.7</sub>Tl<sub>0.2</sub>Mn<sub>0.1</sub>Fe<sup>3+</sup><sub>1.4</sub>Fe<sup>2+</sup><sub>0.2</sub>)(Al<sub>0.2</sub>Si<sub>17.8</sub>)(O<sub>69.0</sub>OH<sub>8.6</sub>F<sub>0.4</sub>); green

in detail. We carried out both bright-field and dark-field imaging in an attempt to locate domains, as well as high-resolution imaging to detect slight differences in schemes of order from one unit cell to the next.

Chemical compositions were obtained by electron-microprobe analysis, and site distributions of  $\text{Fe}^{2+}$  and  $\text{Fe}^{3+}$  were constrained to some extent from analyses of Mössbauer spectra.

#### STRUCTURAL CONSTRAINTS

##### *A means of achieving local charge-balance*

Channels along the 4-fold axes of the  $P4/nnc$  model are critically important to the vesuvianite structure and are the focus of attention in this paper. Within each unit cell, there are two O(10) positions and a string of four cation positions,  $B-C-C-B$ , along each 4-fold axis (Figs. 2, 3). The two adjacent O(10) positions are occupied by oxygen and hydroxyl, with an associated hydrogen bond. Fluorine may locally replace hydroxyl. The  $B-C-C-B$  string usually consists of an alternating sequence of cations and vacancies; in most samples,  $\text{Ca}^{2+}$  occupies the  $C$  positions, and  $\text{Mg}^{2+}$ ,  $\text{Al}^{3+}$ ,  $\text{Fe}^{2+}$ , or  $\text{Fe}^{3+}$  occupy the  $B$  positions.

Adjacent  $B$  and  $C$  positions, 1.3 Å apart, and adjacent  $C$  positions, 2.4 Å apart, are too close to be occupied simultaneously. Thus the occupancy fractions of the  $B$  and  $C$  sites,  $b$  and  $c$ , respectively, are limited to  $0 \leq c \leq 0.5$ , and  $b \leq 1-c$ . If the

$B$  and  $C$  sites are half-filled, with  $b = c = 0.5$ ,  $B$  and  $C$  positions are constrained to be occupied in an alternating manner. These limits on occupancy fractions imply that two  $B$  positions in the same string may be occupied so long as the two adjacent  $C$  positions are vacant.

Notice that the sum of  $b + c$  must be less than or equal to 1. The sum is 1 if every string contains two cations. Strings may occur with only one  $B$  or one  $C$  position occupied and three positions vacant, or perhaps all four positions vacant. Such strings probably occur infrequently because of the disruptive effect they have on local charge-balance on the oxygen atoms in the O(6), O(9), and O(10) positions. Although cations and vacancies are ordered within individual strings, they must be disordered over the  $B$  and  $C$  positions throughout the structure to comply with  $P4/nnc$  symmetry. Most structure analyses of vesuvianite show the  $B$  and  $C$  sites to be close to half-filled, probably because alternate occupancy provides an effective way to satisfy local charge-balance on O(6), O(9), and O(10) oxygen atoms (Allen 1985, Fitzgerald *et al.* 1986b).

Structural and chemical variations in vesuvianite arise primarily from the fact that the  $B$  and  $C$  sites are partly filled. Anions surrounding these sites receive different bond-strength contributions depending on whether a cation or vacancy is present on  $B$  or  $C$ . Local charge-balance may be achieved in two ways: by mixing species of different size or valence on various anionic or cationic sites, or by

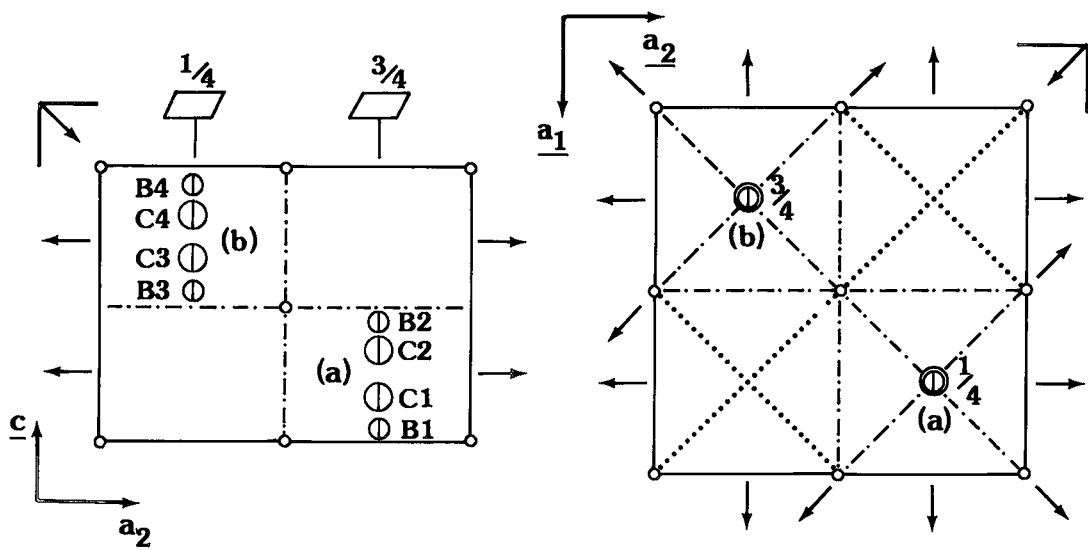


FIG. 2. [100] and [001] projections of the unit cell of vesuvianite showing the distribution of  $B$  and  $C$  positions.  $P4/nnc$  topological symmetry is assumed. (a) and (b) refer to "strings" centered at  $(3/4, 3/4, 3/4)$  and  $(1/4, 1/4, 1/4)$ , respectively.

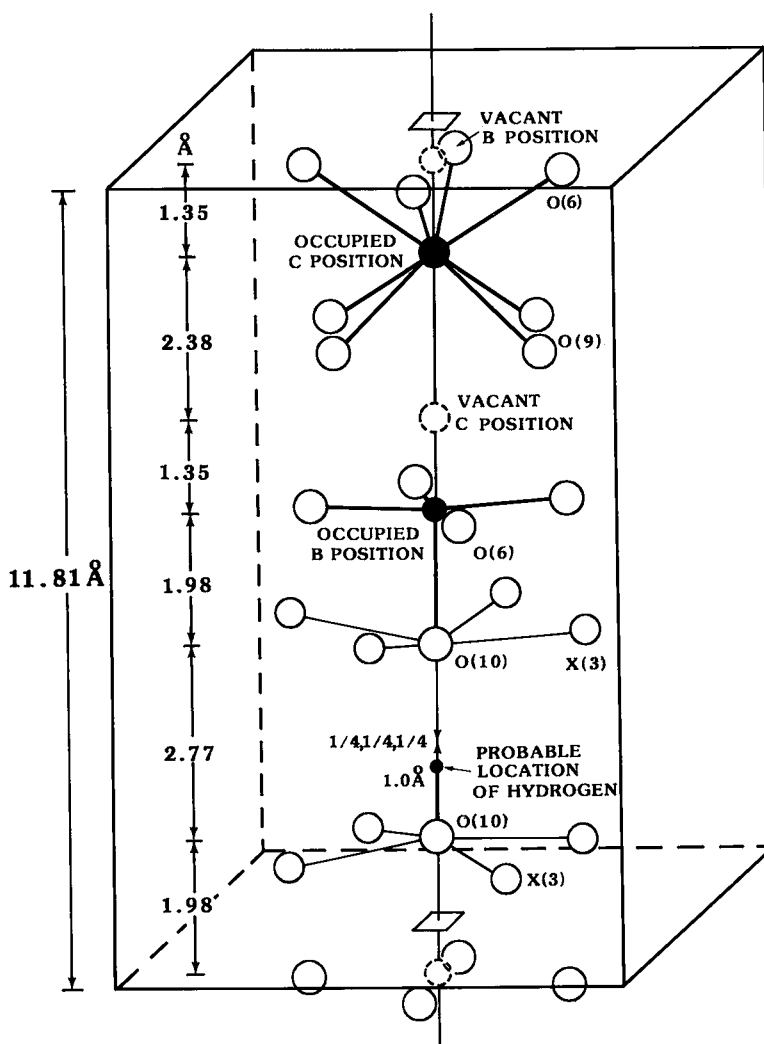
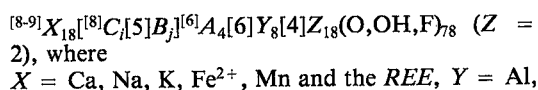


FIG. 3. The atomic arrangement along one of the 4-fold axes in a unit cell of vesuvianite with one C and one B position occupied.

shifting the positions of anions and cations, thereby adjusting effective bond-strengths. In the specific case of the O(10) site, excessive imbalance of charges is prevented by repeating the same string sequence in the *c* direction.

#### Limits on chemical composition

A general formula for vesuvianite based on the *P4/nnc* structure model is:



Mg, Fe<sup>2+</sup>, Fe<sup>3+</sup>, Ca, Ti, Cr, Mn and Zn, Z = Si and Al, A = Al, B = Mg, Al, Fe<sup>2+</sup>, Fe<sup>3+</sup> and Cu, and C = Ca, Na, Fe<sup>2+</sup> and Mn, and where  $0 \leq i \leq 1$ , and  $j \leq 2 - i$ . With the condition that two cations be present per string ( $j = 2 - i$ ), there will be 50 filled cationic sites and two vacancies per formula unit. Half-filled B and C sites correspond to  $i = j = 1$ .

The simplest end-member composition for vesuvianite in the system CaO-MgO-Al<sub>2</sub>O<sub>3</sub>-SiO<sub>2</sub>-H<sub>2</sub>O (CMASH) is Ca<sub>19</sub>MgAl<sub>12</sub>Si<sub>18</sub>O<sub>70</sub>(OH)<sub>8</sub>. Samples with precisely this composition are not known to occur, and a structure having this composition will not be stable because the Pauling

bond-strength sum at O(10) is only 0.89 or 1.29, depending on whether the nearest *B* site is vacant or full. On the other hand, CMASH vesuvianite with nearly this composition has been discovered in rocks from several localities. Samples from Luning, Nevada (Allen & Burnham 1983a, Allen 1985), Asbestos, Quebec (Allen 1985, Fitzgerald *et al.* 1986b), and Georgetown, California (Valley *et al.* 1985, Allen 1985), have compositions close to  $\text{Ca}_{19}\text{Mg}_2\text{Al}_{11}\text{Si}_{18}\text{O}_{69}(\text{OH})_9$ , in which local charge-balance on O(10) is satisfied by a hydrogen bond, absent in the ideal formula.

### Effects of short-range order

The constraint of alternate occupancy of *B* and *C* sites implies short-range order at the unit-cell level in vesuvianite. The string sequence affects the positions of anions and cations surrounding *B* and *C* sites, and gives rise to several schemes of cation-vacancy and positional (CVP) ordering having a variety of  $P4/nnc$  subgroup symmetries. Possibilities having tetragonal symmetry include

$P4/n$ ,  $P4nc$ ,  $P4$ , and  $P4$ . Monoclinic and triclinic subgroups common to both  $P4/n$  and  $P4nc$  include  $P2$ ,  $Pn$  ( $Pc$ ), and  $P1$ .  $P2/n$  and  $P1$  are subgroups of  $P4/n$ , and  $Pnn2$  and  $Pcc2$  are orthorhombic subgroups of  $P4nc$ . For each possible space-group, there are two opposite schemes of atomic order that may be adopted by unit cells (Fig. 4), designated as (+) and (-). Contrasting unit cells having opposite CVP schemes of order are twin-related; the 2-fold rotation axes, glide planes, and inversion center present in supergroup  $P4/nnc$  are used as twin operations (Fig. 5). If unit cells with schemes of order of symmetry lower than tetragonal have metrically tetragonal dimensions, the twinning will be merohedral; if not, then strict merohedry will not exist. In either case, such twinning will be extremely difficult to detect using single-crystal X-ray methods. Nevertheless Veblen & Wiechmann (1991) have observed through TEM a slight splitting of diffraction maxima, which demonstrates a lack of rigorous merohedry, and thereby a scheme of order with less than tetragonal symmetry, probably monoclinic.

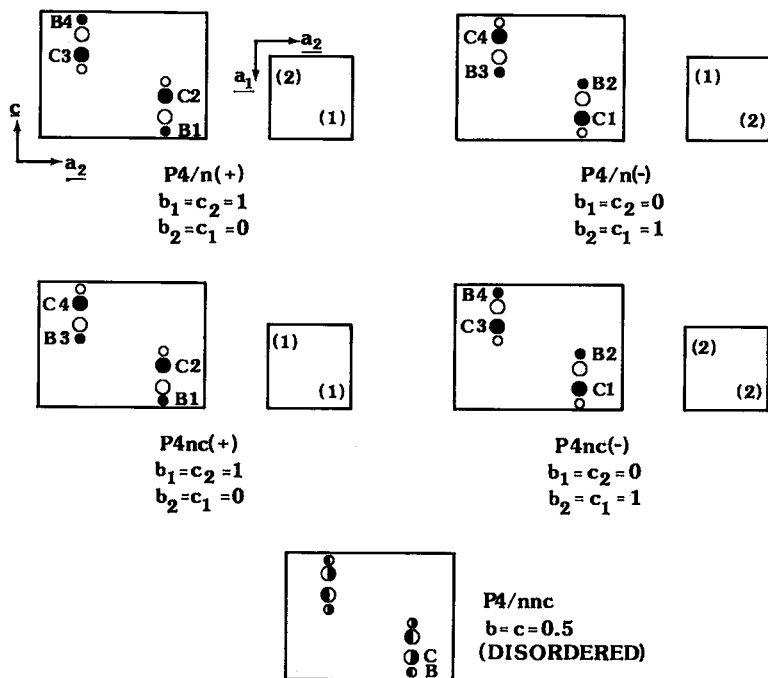
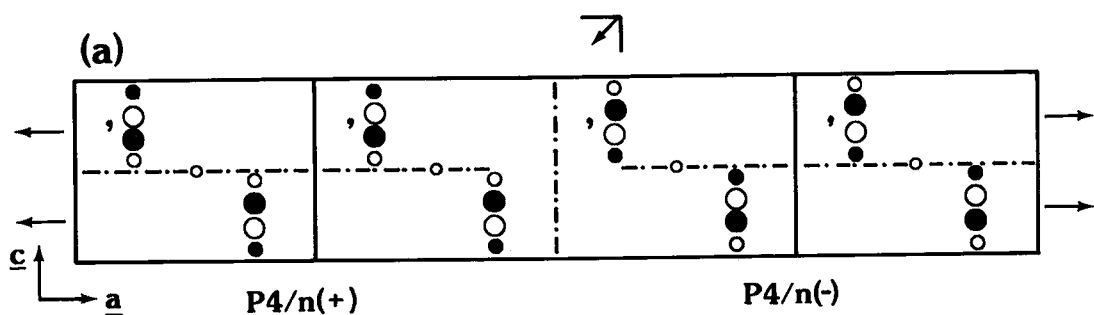
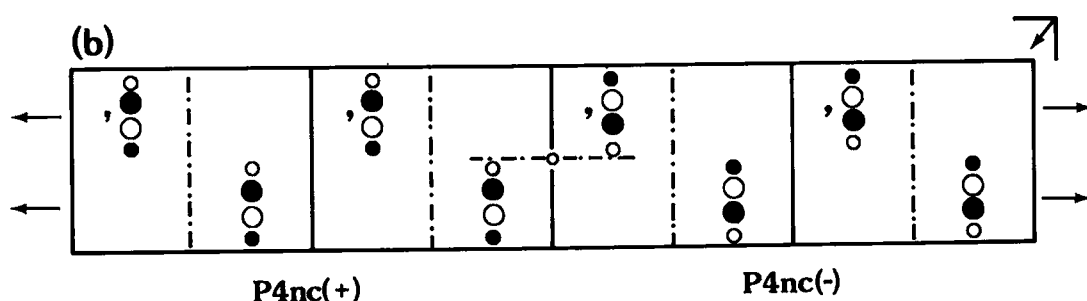


FIG. 4. Four schemes of cation-vacancy ordering based on the alternate occupancy constraint. Site occupancies ( $b_1$ ,  $b_2$ ,  $c_1$ ,  $c_2$ ) are given for the completely ordered arrangements. The symbols (+) and (-) denote "opposite" ordering schemes. Note that space groups  $P4/n$  and  $P4$  have the same possible schemes of cation-vacancy ordering for the *B* and *C* positions. They are distinguished by their schemes of positional order. In  $P4/n$ , the *B* and *C* site symmetry is 4, whereas in  $P4$ , it is 2.



TWIN ELEMENTS: 2-FOLD AXES, (100)  $n$ -GLIDES, (110)  $C$ -GLIDES (NOT SHOWN)



TWIN ELEMENTS: 2-FOLD AXES, (001)  $n$ -GLIDE, INVERSION CENTER

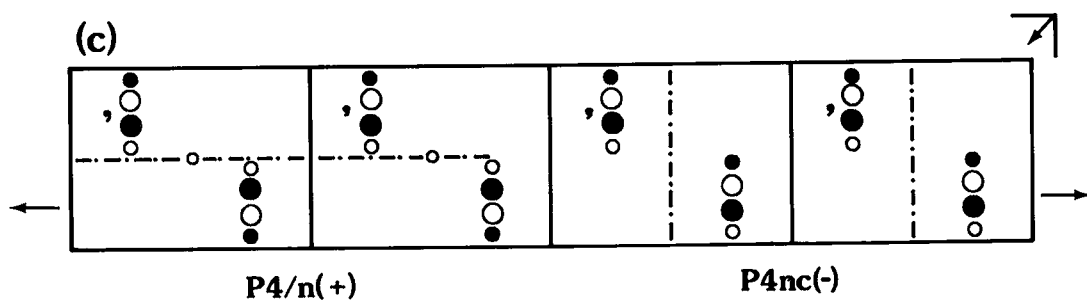


FIG. 5. Twin relationships between oppositely ordered cells. The part of the structure surrounding the strings is nearly consistent with  $P4/nnc$  symmetry. The symbol “,” indicates a change in handedness in opposing quadrants of the cell. Adjacent cells with opposite ordering schemes are related by 2-fold rotation twinning. In (a),  $P4/n(+)$  and  $P4/n(-)$  cells are related by  $n_{(100)}$  and  $c_{(110)}$  glide-plane twinning. In (b),  $P4nc(+)$  and  $P4nc(-)$  cells are related by  $n_{(001)}$  glide-plane twinning and inversion twinning. Adjacent cells with  $P4/n$  and  $P4nc$  ordering schemes in (c) are not twin-related, although parts of the cells are related by 2-fold rotation.

#### HIGH- VERSUS LOW-SYMMETRY VESUVIANITE

##### Basis of symmetry

Two structural forms of vesuvianite are found in nature; they are distinguished on the basis of size of ordered domains: high-symmetry (high)

vesuvianite and low-symmetry (low) vesuvianite (Fig. 6). The diffraction condition used to distinguish high and low vesuvianite is the absence or presence of diffraction maxima that violate glide-plane extinction criteria for space group  $P4/nnc$ . There are three types of glide-violating diffractions (GVDs): type “a”: class  $hk0$  with  $h+k$  odd, type

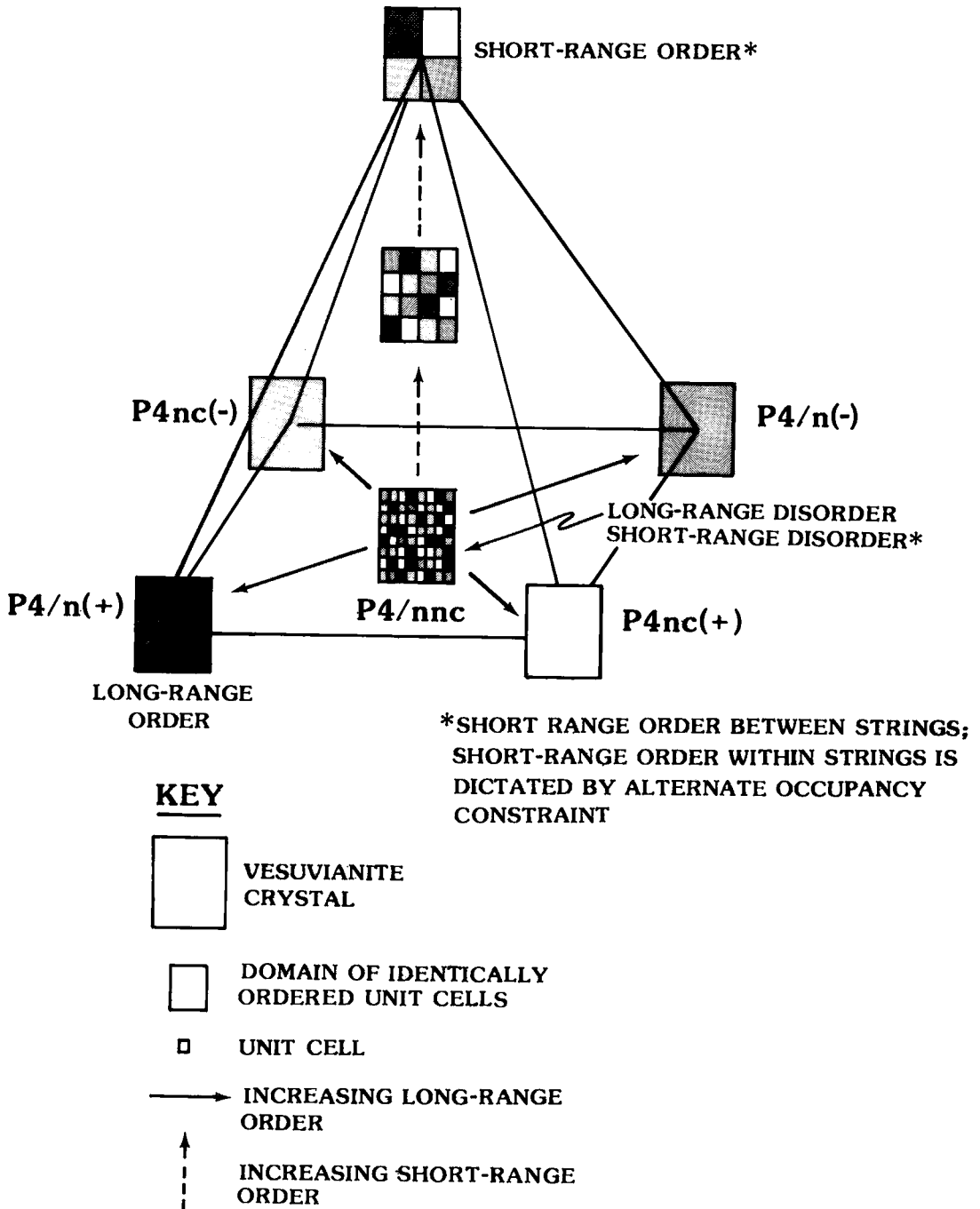


FIG. 6. Possible structures of vesuvianite obtained by varying degrees of long- and short-range order.

“b”: class  $h0l$  with  $h+l$  odd, and type “c”: class  $hhl$  with  $l$  odd.

Diffraction characteristics of vesuvianite samples

from several localities, determined using conventional precession and Weissenberg single-crystal X-ray techniques, are listed in Table 2. Precession

TABLE 2. RELATIVE INTENSITIES OF GVDs ON SINGLE-CRYSTAL X-RAY PHOTOGRAPHS OF VESUVIANITE\*

| Specimen<br>Locality                   | Color                | Type<br>'a'  | Exp.<br>time |     | Type<br>'b' | Exp.<br>time |     | Type<br>'c' | Exp.<br>time |     |   |
|--|----------------------|--------------|--------------|-----|-------------|--------------|-----|-------------|--------------|-----|---|
| <b>METAMORPHIC CALC-SILICATE ROCKS</b> |                      |              |              |     |             |              |     |             |              |     |   |
|  | Sanford, ME          | clove brown  | none         | 72  | w           | none         | 72  | p           | none         | 48  | p |
| A                                      | Sanford, ME          | brown        | none         | 23  | p           | none         | 100 | p           | none         | 104 | p |
|  | Luning, NV           | lt. green    | none         | 48  | w           | none         | 70  | p           | none         | 48  | p |
|  | Lake Jaco, Mex.      | yellow-green | none         | 85  | w           | none         | 71  | p           | none         | 72  | p |
| A                                      | Crestmore, CA        | brown        | none         | 95  | p           | none         | 18  | p           | none         | 143 | p |
| A                                      | Franklin, NJ         | blue         | none         | 67  | p           | weak         | 119 | p           | weak         | 96  | p |
| A                                      | Franklin, NJ         | pink         | none         | 19  | p           | none         | 22  | p           | none         | 22  | p |
| A                                      | Telemark, Nor.       | blue         | none         | 94  | p           | weak         | 53  | p           | weak         | 45  | p |
| A                                      | Wilui R., USSR       | green        | none         | 90  | p           | none         | 94  | p           | none         | 94  | p |
| A                                      | Antamina, Peru       | yellow       | none         | 30  | p           | none         | 14  | p           | none         | 23  | p |
| A                                      | Monte Somma, Italy   | brown        | none         | 100 | p           | weak         | 79  | p           | weak         | 85  | p |
| <b>RODINGITES</b>                      |                      |              |              |     |             |              |     |             |              |     |   |
|  | Eden Mills, VT       | olive green  | none         | 72  | w           | strong       | 48  | p           | strong       | 48  | p |
| A                                      | Eden Mills, VT       | green        | none         | 55  | p           | strong       | 29  | p           | strong       | 19  | p |
|  | Asbestos, QC         | colorless    | none         | 24  | w           | strong       | 30  | w           | strong       | 30  | w |
|  | Asbestos, QC         | pale green   | none         | 24  | w           | strong       | 24  | p           | strong       | 24  | p |
| A                                      | Asbestos, QC         | pale green   | weak         | 159 | p           | strong       | 39  | p           | strong       | 25  | p |
| A                                      | Coleraine, QC        | lilac        | none         | 98  | p           | strong       | 15  | p           | strong       | 30  | p |
| A                                      | Black Lake, QC       | brown        | none         | 20  | p           | strong       | 26  | p           | strong       | 18  | p |
| A                                      | Laurel, QC           | yellow       | none         | 72  | p           | strong       | 95  | p           | strong       | 70  | p |
|  | Georgetown, CA       | yellow       | none         | 24  | w           | v. strong    | 48  | p           | v. strong    | 43  | p |
| A                                      | Georgetown, CA       | green        | weak         | 61  | p           | strong       | 9   | p           | strong       | 11  | p |
| A                                      | Hindubagh, Pak.      | green        | weak         | 106 | p           | strong       | 50  | p           | strong       | 57  | p |
| <b>ALTERED ALKALI SYENITES</b>         |                      |              |              |     |             |              |     |             |              |     |   |
|  | Dungannon Twp., Ont. | brown        | none         | 72  | p           | weak         | 72  | p           | weak         | 72  | w |
|  |                      |              |              |     |             | weak         | 48  | p           |              |     |   |
| A                                      | San Benito Co., CA   | brown        | weak         | 44  | p           | strong       | 56  | p           | strong       | 66  | p |

\* Exposure time in hours. Key: A = results from Arem (1970), w = Weissenberg photo, p = precession photo.

data from Arem & Burnham (1969) and Arem (1970) are included in this table for comparison. GVDs are generally seen in vesuvianite samples from rodingites and altered alkali syenites, but not in vesuvianite from metamorphic calc-silicate rocks. In several precession photographs, many strong "b" and "c" diffraction maxima are observed; in others, there are only a few weak "b" and "c" diffractions. Arem (1970) detected weak "a" diffraction maxima in very-long-exposure precession photographs of several samples, but Allen (1985) has demonstrated that most, if not all, "a" diffractions are a consequence of multiple diffraction (Renninger effect).

Failure to observe GVDs in X-ray photographs of vesuvianite should not be construed as unequivocal proof that the crystal possesses glide-plane symmetry, since longer exposures may reveal violations. The labels "high" and "low" must

therefore be qualified. We consider a sample to be high vesuvianite if no glide violations are observed on X-ray photographs exposed for 24 to 72 hours. Weak violations may be detected on diffractometer records or on photographs exposed for longer than 72 hours. Low vesuvianite, on the other hand, exhibits relatively intense and pervasive glide-plane violations even on X-ray photographs exposed 12 to 24 hours.

The context of the terms "strong" and "weak" in reference to the intensities of GVDs may be seen from 4-circle X-ray diffractometer measurements of low vesuvianite crystals from Asbestos, Georgetown, and Eden Mills. The presence of "b" and "c" diffraction maxima was confirmed. Extremely weak "a" diffraction maxima also were detected, but because they show variable intensities in psi-scans, they were considered to have arisen from multiple diffraction. From the intensities and

TABLE 3. INTEGRATED INTENSITIES OF FUNDAMENTAL AND GLIDE-VIOLATING DIFFRACTIONS FOR THREE SAMPLES OF LOW VESUVIANITE\*

| <i>hkl</i> | Asbestos, QC |            | Georgetown, CA |            | Eden Mills, VT |            |
|------------|--------------|------------|----------------|------------|----------------|------------|
|            | <i>I</i>     | $\sigma_1$ | <i>I</i>       | $\sigma_1$ | <i>I</i>       | $\sigma_1$ |
| 004        | 100.0        | 0.44       | 100.0          | 0.37       | 100.0          | 0.63       |
| 440        | 34.99        | 0.16       | 36.52          | 0.22       | 35.53          | 0.38       |
| 'a' 230    | 0.01         | 0.01       | 0.01           | 0.003      | 0.01           | 0.01       |
| 'b' 104    | 0.38         | 0.01       | 0.78           | 0.02       | 0.58           | 0.02       |
| 'c' 223    | 0.24         | 0.01       | 0.62           | 0.02       | 0.44           | 0.02       |

\* Intensities are given relative to that for 004.

standard deviations of 004, 440, 230, 104, and 223 diffractions for the three samples (Table 3), the relative weakness of the GVDs is clear. The intensities of the strongest "b" and "c" diffractions in the entire diffractometer record (104 and 223) are about three orders of magnitude less than that of the most intense diffraction. Such weakness of GVDs is not particularly surprising, because the substitutional ordering responsible for their origin involves only the 4 atoms on *B* and *C* positions out of 256 total atoms per unit cell. Positional ordering also may contribute to the intensities of GVDs, but the atomic displacements are so small that the net effect is insignificant.

Other experimental evidence supports the use of X-ray diffraction to distinguish between high and low vesuvianite. Results from second-harmonic analysis (SHG), for example, show high vesuvianite to be centric and low vesuvianite to be acentric (Table 4). Furthermore, polarized-light microscopy reveals non-uniaxial behavior in both forms.

### High vesuvianite

High vesuvianite is found in skarns, calc-silicate hornfels, and calc-schists, where it formed at relatively high temperatures (400–800°C). High vesuvianite exhibits *P4/nnc* average symmetry, which suggests long-range disorder with respect to the cation-vacancy distribution in *B* and *C* sites and to the position of anions and cations surrounding the *B* and *C* positions. All structure refinements of high vesuvianite reported over the past 20 years (Coda *et al.* 1970, Rucklidge *et al.* 1975, Allen & Burnham 1983a, Allen 1985, Fitzgerald *et al.* 1986a, Yoshiasa & Matsumoto 1986) show that the *B* and *C* sites are statistically half occupied and that positional disorder leads to high temperature-factors. Short-range order must exist at the unit-cell level because of the alternate occupancy constraint. Identically ordered unit-cells may form chains along *c* to maintain local charge-balance on the O(10) oxygen atoms. High vesuvianite typically exhibits overall tetragonal symmetry, no GVDs, a null SHG signal, a uniaxial interference figure, and fine-scale lamellar and cross-hatch twinning (Fig. 7).

TABLE 4. SHG RESULTS FOR VESUVIANITE SAMPLES\*

| Specimen Locality                      | SH(+0) <sup>1</sup> | vfs <sup>2</sup> | N <sup>3</sup> | Remarks            |
|--|---------------------|------------------|----------------|--------------------|
| <b>METAMORPHIC CALC-SILICATE ROCKS</b> |                     |                  |                |                    |
| Sanford, ME                            | 0                   | 1                | 4              | powder (brown)     |
| "                                      | 0                   | 1                | 1              | (001) section      |
| Poland, ME                             | 0                   | 0.2              | 2              | powder (brown)     |
| Robinson Mtn., ME                      | 0                   | 1                | 2              | powder (brown)     |
| "                                      | 0                   | 1                | 1              | (001) section      |
| Warren, NH                             | 0                   | 1                | 2              | powder (brown)     |
| Mt. Vesuvius, Italy                    | 0                   | 0.4              | 2              | powder (dk. green) |
| Monte Somma, Italy                     | 0                   | 0.2              | 2              | powder (dk. green) |
| Crestmore, CA (H)                      | + w                 | 1                | 3              | powder (lt. green) |
| "                                      | 0                   | 1                | 3              | xtal. frag.        |
| Magnet Cove, AR                        | 0                   | 0.4              | 2              | powder (lt. green) |
| Wilul River, USSR (H)                  | 0                   | 1                | 2              | powder (dk. green) |
| Olmsteadville, NY                      | 0                   | 1                | 2              | powder (brown)     |
| Frugard, Finland                       | 0                   | 1                | 2              | powder (brown)     |
| Lake Jaco, Mexico                      | 0                   | 1                | 3              | powder (yellow)    |
| Telemark, Norway (H)                   | 0                   | 1                | 4              | powder (blue)      |
| "                                      | 0                   | 1                | 3              | xtal. frag.        |
| Franklin, NJ (H)                       | 0                   | 1                | 3              | powder (blue)      |
| <b>RODINGITES</b>                      |                     |                  |                |                    |
| Asbestos, QC (L)                       | + m                 | 1                | 3              | powder (lt. green) |
| "                                      | + m                 | 1                | 2              | (001) section      |
| Eden Mills, VT (L)                     | + m                 | 1                | 6              | powder (green)     |
| "                                      | + vs                | 10               | 6              | (001) section      |
| "                                      | + vs                | 10               | 2              | (100) section      |
| "                                      | + vs                | 10               | 3              | (110) section      |
| Georgetown, CA (L)                     | + m                 | 1                | 6              | powder (yellow)    |
| "                                      | + w                 | 1                | 3              | grains (clear)     |
| "                                      | + w                 | 1                | 3              | grains (violet)    |
| "                                      | + s                 | 1                | 3              | grains (green)     |
| "                                      | + s                 | 1                | 3              | grains (yellow)    |
| "                                      | + s                 | 1                | 3              | grains (dark red)  |
| Hindubagh, Pakistan                    | + s                 | 1                | 2              | powder (green)     |
| "                                      | + s                 | 1                | 2              | xtal. frag.        |
| <b>ALTERED ALKALI SYENITES</b>         |                     |                  |                |                    |
| Sewards Penn., AK                      | 0                   | 1                | 2              | powder (black)     |
| "                                      | 0                   | 1                | 1              | xtal. frag.        |
| Dungannon Twp., ON (L)                 | 0                   | 1                | 2              | powder (brown)     |
| "                                      | 0                   | 1                | 2              | xtal. frag.        |

\* Data collected at Materials Research Laboratory, Pennsylvania State University.  
Key: H = high vesuvianite, L = low vesuvianite.

<sup>1</sup> Second harmonic (SHG) signal is either positive (+) or null (0). Relative intensity of SHG signal: 'w' = weak, 'm' = medium, 's' = strong, 'vs' = very strong.

<sup>2</sup> vfs = volts full scale on digital oscilloscope.

<sup>3</sup> N = number of repetitions.

The Luning high vesuvianite has a nearly pure CMASH composition:  $\text{Ca}_{18.8}(\text{Al}_{10.3}\text{Mg}_{2.6}\text{Fe}_{0.3})(\text{Al}_{0.4}\text{Si}_{17.6})(\text{O}_{68.3}\text{OH}_{9.3}\text{F}_{0.4})$ . All the other samples of high vesuvianite whose structures have been refined are iron-bearing; the Franklin samples also contain Cu and Zn.  $\text{Fe}^{2+}$  and  $\text{Fe}^{3+}$  both occur in varying amounts and occupy either the *X*, *Y*, *B*, or *C* sites. Site assignments are therefore difficult to make based on X-ray data alone. Although the interpretation of Mössbauer spectra hinges critically on the crystal chemical assumptions made, Allen (1985) has used such data successfully to determine cation distributions more accurately.

### Low vesuvianite

Low vesuvianite is found in veins, in rodingites, and in altered alkali syenites. The vein material is commonly of gem quality. Low vesuvianite forms

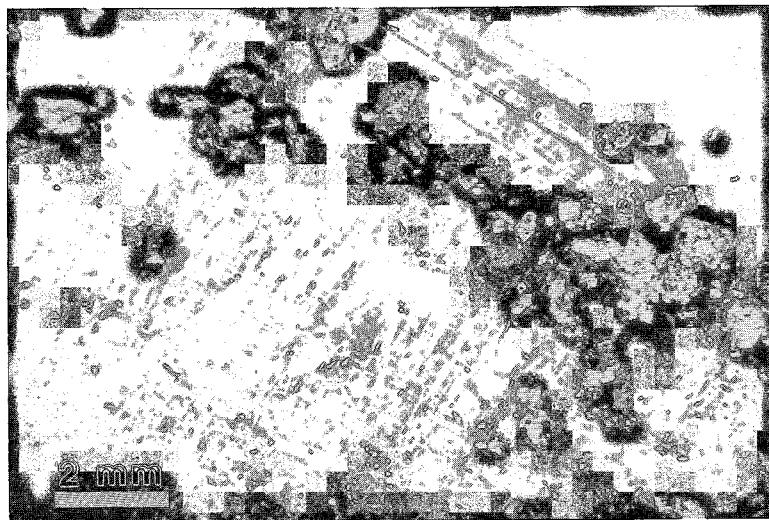


FIG. 7. Cross-hatch twinning in (001) section of high vesuvianite from Luning, Nevada.

at temperatures below 300°C as a product of hydrothermal alteration or deposition. The essential difference between high and low vesuvianite is the presence of resolvable domains in the latter. These multicell domains imply short-range order beyond the unit-cell level caused by interactions between strings that lead to a predominant CVP scheme of order. Differently ordered domains may be perfect or imperfect and are related by merohedral, or nearly merohedral, twinning, depending on whether or not they are dimensionally tetragonal.

If a crystal contains equal volumes of oppositely ordered domains, the average structure exhibits  $P4/nnc$  pseudosymmetry, but GVDs manifest the lower symmetry of the ordered domains. If a crystal contains unequal volumes of oppositely ordered domains, the average symmetry will depend on the preferred CVP scheme of order.

Some samples of low vesuvianite exhibit cell parameters consistent with tetragonal symmetry, but others seem to have nontetragonal parameters ( $a_1 \neq a_2$ ) (see Table 5, also Veblen & Wiechmann 1991). Positive SHG results indicate that some or all of the domains in low vesuvianite have symmetry consistent with one of the acentric subgroups,  $P\bar{4}$  or  $P4nc$ , or lower subgroups. Such samples usually exhibit biaxial interference figures and anomalous birefringence in (001) sections, further indicating symmetry lower than tetragonal. Growth sectors are commonly evident (Fig. 8).

Structure refinements of low vesuvianite have been reported only recently. Giuseppetti & Mazzi

(1983) refined the structure of low vesuvianite from Italy in space group  $P4/n$ . Samples from the following rodingite localities also have been refined: Georgetown, California, in space group  $P4/nnc$  (Valley *et al.* 1985, Allen 1985), Asbestos, Quebec, in  $P4/nnc$  (Allen 1985) and  $P4/n$  (Fitzgerald *et al.* 1986b); and Eden Mills, Vermont, in  $P4/n$  and  $P\bar{4}$  (Allen & Burnham 1983b, Allen 1985). A REE-bearing sample from an altered alkali syenite in San Benito County, California was refined in  $P4/n$  (Fitzgerald *et al.* 1987).

Nearly pure CMASH samples examined by Allen (1985) from Asbestos,  $\text{Ca}_{18.9}(\text{Al}_{11.1}\text{Mg}_{1.9}\text{Fe}_{0.1})(\text{Si}_{18.0}\text{O}_{69.2}\text{OH}_{8.6}\text{F}_{0.2})$ , and Georgetown,  $\text{Ca}_{19.0}(\text{Al}_{10.8}\text{Mg}_{1.8}\text{Fe}_{0.4})(\text{Al}_{0.1}\text{Si}_{17.9})(\text{O}_{69.1}\text{OH}_{8.7}\text{F}_{0.2})$ , had to be refined assuming  $P4/nnc$  pseudosymmetry. Valley *et al.* (1985) had to do the same with their Georgetown sample. Results showed that the  $B$  and

TABLE 5. HIGH-PRECISION CELL PARAMETERS FOR VESUVIANITE FROM EDEN MILLS AND LUNING\*

|   |                            |
|---|----------------------------|
| Eden Mills low vesuvianite                              |                            |
| 98 observations; $hkl$ , $kh0$ , and $hhl$ diffractions |                            |
| $a_1$   | = 15.5498(4) Å             |
| $a_2$   | = 15.5594(5) Å             |
| $c$   | = 11.8276(6) Å             |
| $V$   | = 2861.6(2) Å <sup>3</sup> |
| Luning high-vesuvianite                                 |                            |
| 50 observations; $hkl$ and $kh0$ diffractions           |                            |
| $a_1 = a_2$   | = 15.562(1) Å              |

\* Data obtained from refinements of back-reflection Weissenberg measurements. Standard deviations in parentheses.

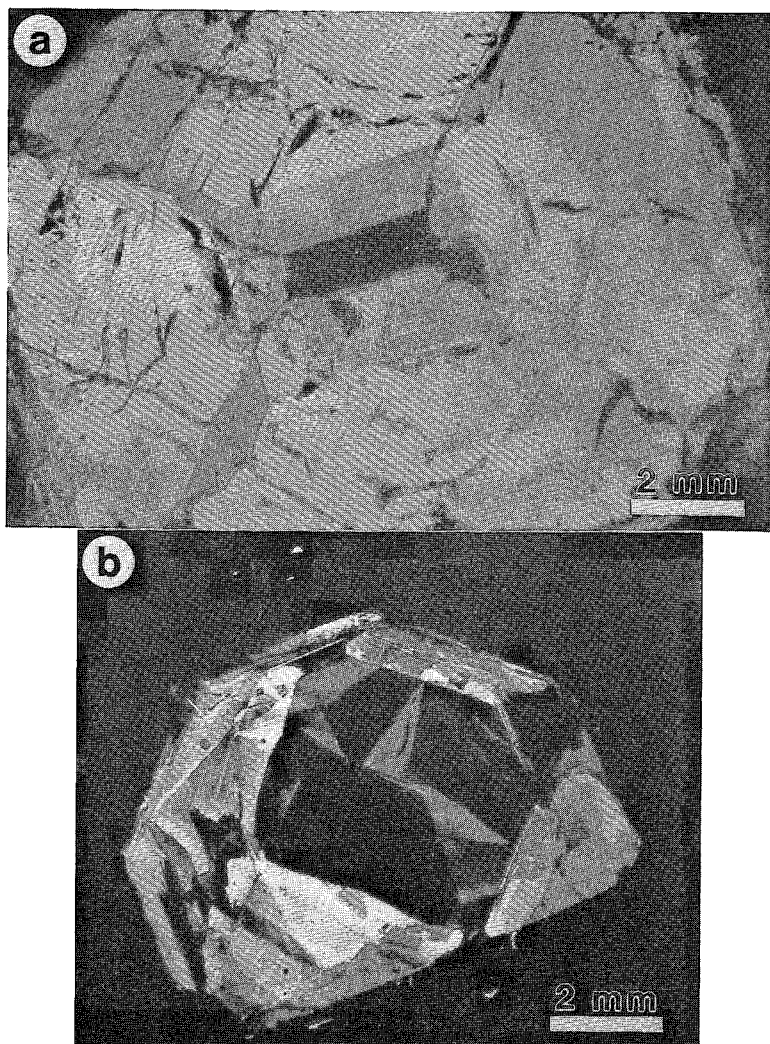


FIG. 8. Sectoral structure in (001) section of low vesuvianite from (a) Eden Mills, Vermont and (b) Asbestos, Quebec.

C sites are half-filled on average, which implies long-range cation-vacancy disorder; positional disorder was indicated by high temperature-factors.

The iron-bearing Eden Mills sample,  $\text{Ca}_{19.0}(\text{Al}_{9.4}\text{Mg}_{1.7}\text{Ti}_{0.2}\text{Mn}_{0.1}\text{Fe}_{1.6})(\text{Al}_{0.2}\text{Si}_{17.8})(\text{O}_{69.2}\text{OH}_{8.4}\text{F}_{0.4})$ , exhibits incomplete long-range order, with a preference for  $P4/n$  or  $P4$  ordering. Cation-vacancy ordering leads to topochemical distinctions among the B and C sites; B1 and C2 contain 70% (Fe, Mg) and Ca, respectively, versus 30% for B2 and C1 (Fig. 4). The refinement results show positional order that is more consistent with  $\bar{P}4$  than with  $P4/n$ , which could account for the positive SHG signal.

Giuseppetti & Mazzi (1983) reported site oc-

cupancies for their low vesuvianite that indicate incomplete long-range order consistent with  $P4/n$ . Fitzgerald *et al.* (1986b, 1987) did not report refined B1, B2, C1, and C2 site occupancies with their  $P4/n$  structure models of low vesuvianite from Asbestos and San Benito. The existence of ordered domains in low vesuvianite was first suggested by Giuseppetti & Mazzi (1983) and Allen & Burnham (1983b), but their presence has been confirmed by experiment only recently. Allen (1985) suggested that the domains are columnar in shape, elongate parallel to  $c$ , as indicated by the orientation of streaks of very weak diffuse intensity associated with GVDs. In selected-area electron-diffraction (SAED) patterns, the GVDs are usually seen as diffuse streaks

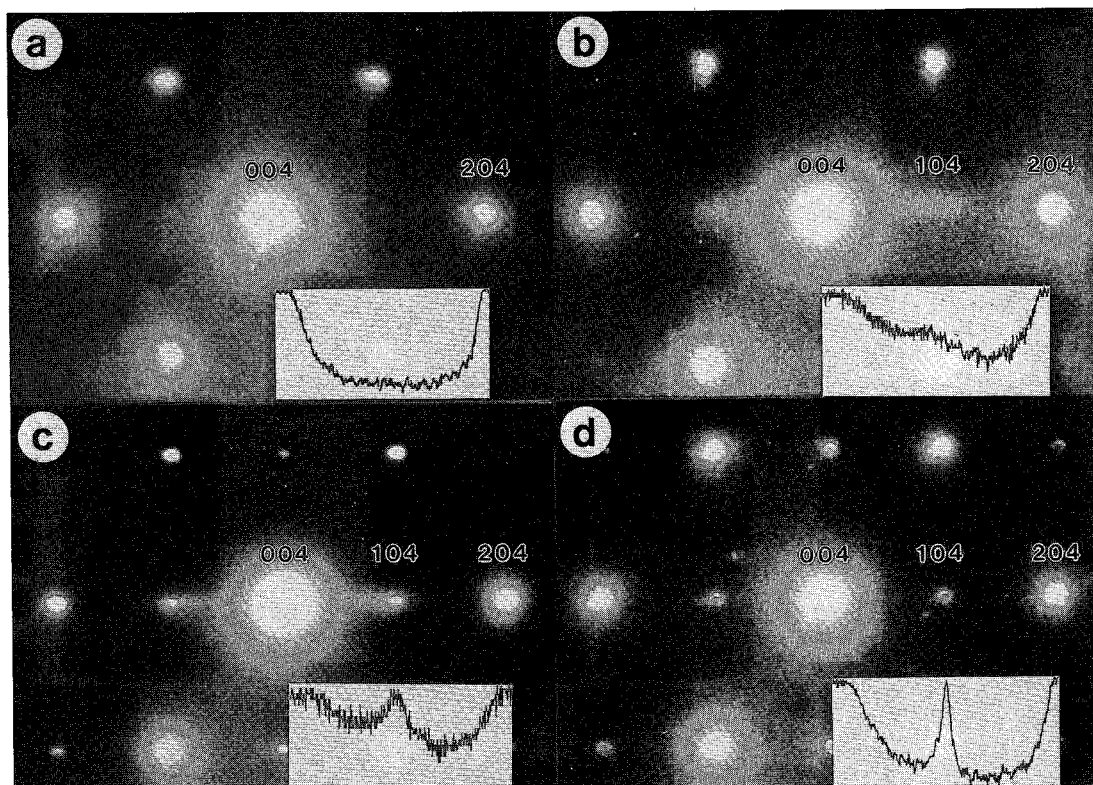


FIG. 9. Overexposed SAED patterns of high vesuvianite from (a) Sanford and (b) Luning, and low vesuvianite from (c) Eden Mills and (d) Asbestos. Insets show trace of diffracted intensity along  $a^*$  between 004 and 204. The Sanford sample shows no glide-violating ("b") diffractions. The Luning sample shows diffuse intensity along  $a^*$  but no sharp spot in the Bragg position of GVDs (e.g., 104). The Eden Mills sample shows diffuse streaking along  $a^*$  associated with sharp GVDs. Finally, the Asbestos sample shows spots but no streaking. The orientation of the streaks implies short-range order in the  $a$  direction of crystals. Note that the fundamental diffractions (e.g., 004, 204) are always sharp.

flattened along  $c^*$ , with a sharp spot at the center in the Bragg position.

Using dark-field and high-resolution TEM imaging, Veblen & Wiechmann (1991) observed fine-scale domains in vesuvianite from Crestmore, California. The domains are 10–50 nm in size and are elongated parallel to  $c$ . Larger domains that exceed 1  $\mu$ m in size also are seen in some areas. The pervasive domain-structure in this sample is believed to have formed by transformation twinning, the result of ordering of a disordered high vesuvianite.

Overexposed SAED patterns of high and low vesuvianites from several localities (Fig. 9) show differences in the appearance of GVDs. They are seen as diffuse streaks, sharp spots, or combinations of the two. However, no evidence of a domain structure is seen in dark-field TEM images because of the relative weakness of these diffracted beams.

In general, the fine-scale variation in the degree of ordering between domains is simply too slight to detect even in high-resolution TEM structure images. Substitutional differences involve only a small number of atoms per cell, and positional displacements are only on the order of a few hundredths of an Ångström.

Columnar domains probably form because ordering along  $c$  leads to attainment of local charge-balance on the O(10) oxygen atoms (Fig. 10). Short-range ordering in the  $a$  and [111] directions presumably occurs because of indirect string-string interactions. The sequence of one string in a unit cell influences the scheme of positional order, which in turn affects the sequence of a neighboring string within the same cell or an adjacent cell. The continuity of this indirect communication between strings presumably determines the size of domains.

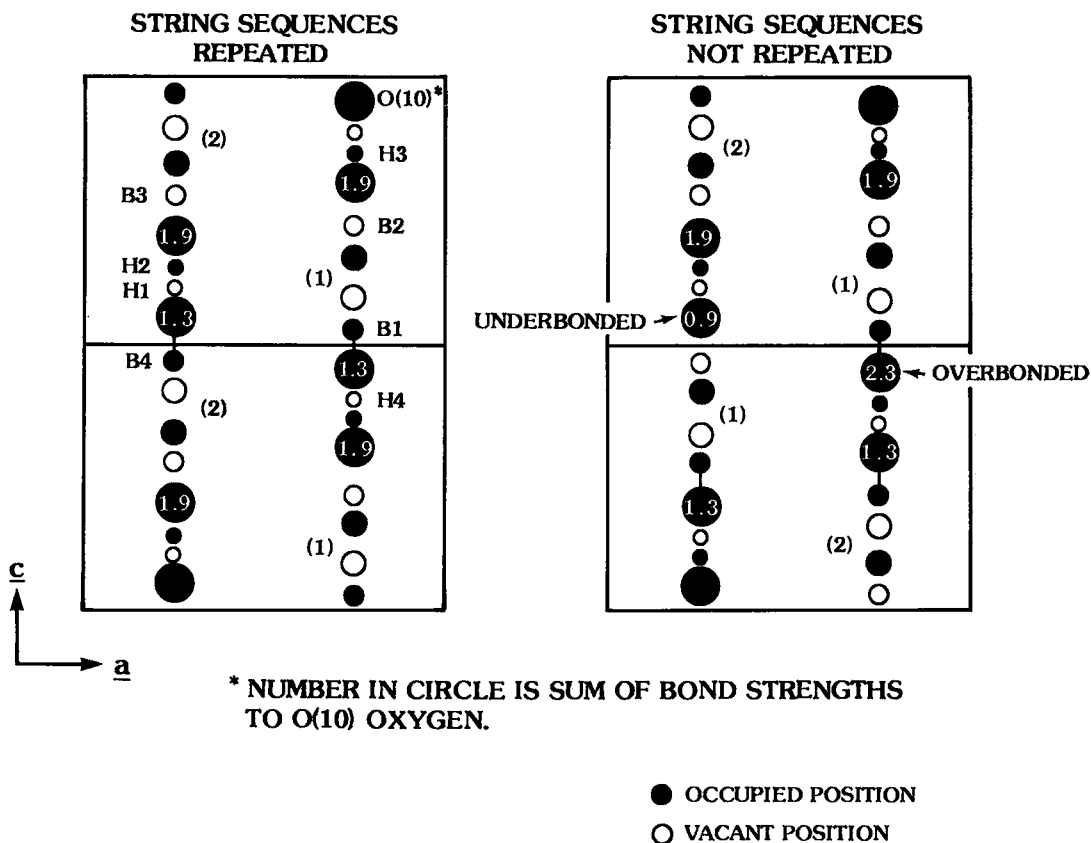


FIG. 10. Cation-vacancy and hydrogen-vacancy ordering in the  $c$  direction in vesuvianite. The impetus for ordering is the attainment of local charge-balance on the O(10) oxygen. The pair of cells on the left shows that local charge-balance is achieved if string sequences are repeated along  $c$ . The pair of cells on the right shows that local charge-balance is disrupted if string sequences vary along  $c$ .

### Structure energetics of ordering

Domains based on different CVP schemes of order have very similar structures, making them nearly equivalent energetically. Structure-energy calculations, made using a modified version of WMIN (Busing 1981) following procedures described by Post & Burnham (1986), yield identical structure energies (-1262.3 kcal/oxygen atom) for the  $P4/n$  and  $P4nc$  (both + and -) schemes of order, based on refined atomic coordinates from a  $P4/nnc$  refinement. On the other hand, the structure energy calculated for the  $P4/n(-)$  CVP antiordered scheme using refined  $P4/n(+)$  coordinates of ordered atoms for the Eden Mills sample is greater than that for the  $P4/n(+)$  scheme of order by 5.9 kJ/oxygen atom (-5281.5 kJ/oxygen versus -5275.6 kJ/oxygen), which is a very significant difference, corresponding to 460

kJ/mole. Thus, although these calculations provide neither an order-antioder interchange energy nor an energy of disordering, they do suggest that various schemes of order have atom configurations that are energetically distinct, and that the existence of a particular scheme of order along one string will influence the choice of scheme in nearby strings, thus providing some impetus for formation of short-range ordered domains.

Changes in the CVP scheme of order may take place while a crystal is growing if the growth conditions are perturbed slightly. It would therefore not be surprising to find crystals containing differently ordered domains. The crystals of low vesuvianite from Asbestos and Georgetown refined by Allen (1985) presumably contain approximately equal volumes of oppositely ordered domains. On the other hand, a period of uninterrupted growth at a constant low temperature might promote

long-range order. The low vesuvianite from Eden Mills possesses partial long-range order and contains unequal volumes of oppositely ordered domains, indicating a preference for one of the CVP schemes of order.

Disordered CVP arrangements will be favored if their Gibbs free energy,  $G = H - TS$ , is lower than that of ordered states. Under the (not unreasonable) assumptions that the molar volumes and heat capacities of ordered and disordered states are essentially the same, disorder will prevail at temperatures where  $T\Delta S_{\text{config}}$  is greater than the undoubtedly positive difference in structure energy,  $\Delta E_{\text{disorder}}$ . With respect to cation distributions in the *B* and *C* sites, our model assumes that crystal-chemical constraints require ordering along individual B-C-C-B strings, and that the disorder can be described as a random arrangement of ordered strings. If this is the case, the configurational entropy,  $S_{\text{config}}$ , of disordered arrangements of strings will not be calculated in the same way as for standard site-disorder, but rather will depend on the total number of strings per mole of crystal. Following the arguments of Thompson (1981), who discussed the analogous problem relative to  $S_{\text{config}}$  for stacking disorder in micas, a mole of vesuvianite can only be disordered if it contains more than one string. The configurational entropy will be given by [Thompson 1981, Eq. (1)]

$$S_{\text{config}} = -kn \sum N_i \ln N_i$$

where  $k$  is the Boltzmann constant,  $n$  is the total number of strings, and  $N_i$  is the fraction of strings with order of type  $i$ . From our previous discussion, it is reasonable to assume that for net *B*- and *C*-site occupancies of 0.5, there can be two distinct types of ordered strings (Fig. 4). The maximum configurational entropy will obtain when the number of strings per mole of crystal is maximized. In one mole of vesuvianite, the greatest number of strings will occur if the crystal is a sheet parallel to (001) only one unit cell thick. Since  $Z = 2$  and there are two strings per unit cell, one mole of such a crystal will contain one mole of strings and will cover an area of about 0.7 km<sup>2</sup>. Assuming a random distribution of equal numbers of the two types of ordered strings, our absurdly shaped crystal would have a configurational entropy given by

$$S_{\text{config}} \text{ (per mole of strings)} = R \ln 2$$

or 5.76 JK<sup>-1</sup>mole<sup>-1</sup>. As the number of (001) layers in our crystal increases, the number of strings and  $S_{\text{config}}$  remain constant, but  $S_{\text{config}}$  per unit mass decreases. Thus whereas structure energy per unit mass is constant,  $S_{\text{config}}$  per unit mass decreases as crystal length/width ratio increases (length

measured along *c*). Disordered crystals with length/width ratios in the usual range of, say, 1 to 5, will have minuscule configurational entropies, less than  $1 \times 10^{-10}$  JK<sup>-1</sup>mole<sup>-1</sup>.

The inevitable conclusion is that equilibrium disorder of B-C-C-B strings alone will never be favored at any geologically reasonable temperature, unless the enthalpy of disordering,  $\Delta H_{\text{disorder}}$ , is as minuscule as  $T\Delta S_{\text{config}}$  is likely to be for reasonably shaped crystals. If the energy of disordering,  $\Delta E_{\text{disorder}}$ , is of a similar order of magnitude, the  $P\Delta V_{\text{disorder}}$  term will be important, even at atmospheric pressure. Unfortunately, none of these thermochemical values are readily accessible either experimentally or theoretically at present. This analysis, we believe, supports our assertion that the state of order or disorder displayed by B-C-C-B strings in any sample of vesuvianite is likely to be most dependent on specific conditions of growth rather than on equilibrium thermodynamic considerations. If, however, disordering of Al-Si on *Z* sites, Al-(Mg,Fe,Ti) on *Y* sites, Ca-Na on *X* sites, or OH-F also occurs, the substantially greater  $S_{\text{config}}$  may indeed stabilize disordered structural states at high metamorphic temperatures, and CVP string disorder may well accompany the site disorder.

#### THE GROWTH HISTORY OF VESUVIANITE

High vesuvianite is the product of contact and regional metamorphism, with or without metasomatic activity. It is formed essentially by diffusion of chemical components in impure limestones, due to a gradient in temperature or chemical potential (or both). In most reported cases, high vesuvianite is formed by prograde reactions, generally in the temperature range of 400–800°C.

Low vesuvianite, on the other hand, typically is the product of late-stage hydrothermal processes (alteration and deposition) accompanied by metasomatic activity. It either replaces existing minerals *via* retrograde reactions, as in rodingites and alkali syenites, or is precipitated directly from freely moving solutions to form veins. These occurrences presumably form at temperatures below 300°C, as suggested by the presence of other low-temperature minerals such as hydrogrossular, prehnite, chlorite, and xonotlite, in addition to chrysotile and lizardite in the surrounding serpentinite.

The fact that low vesuvianite is found in rocks formed at low temperatures suggests that ordering occurred during, not after, crystal growth. Limited short-range ordering presumably took place as the crystal grew metastably in a hydrothermal environment characterized by fairly rapid rates of growth.

The ordered structure was determined by the two-dimensional atomic arrangements exposed on the surface at the time the crystal was growing, and was frozen during and after growth. Sectors were formed as the degree of order (or the ordering scheme itself) varied during growth. Crystals exhibit anomalous optical properties because of the reduced symmetry of individual sectors.

Metastable growth involving limited ordering is observed in other minerals that also occur in low-temperature regimes. Sectors in birefringent grandite garnet, for example, are formed by varying degrees of Al-Fe<sup>3+</sup> order on the octahedral positions, causing a reduction in symmetry from cubic to triclinic (Takéuchi *et al.* 1982, Allen & Buseck 1988). Akizuki (1984) found a correlation between surface features and internal textures and suggested that the optical anomalies in birefringent garnet are produced by Al-Fe<sup>3+</sup> ordering during crystal growth and not by a transformation after growth. Topaz also shows a sectoral structure formed during growth (Akizuki *et al.* 1979). Anomalous optical properties observed within the sectors are considered to result from an ordered distribution of fluorine and hydroxyl.

Akizuki (1987) has proposed a general mechanism for formation of growth sectors based on studies of the relationships between surface features and internal textures of Al-bearing silicates such as prehnite, feldspars, and zeolites. Optical variations in these minerals are explained by differences in Al-Si order established during growth. In vesuvianite, the situation is substantially more complicated because ordering may involve ions on several different sites: Al-Si (*Z* sites); Al-(Mg,Fe,Ti) (*Y* sites); Ca-Na (*X* sites); (Al,Mg)-vacancy (*B* site); Ca-vacancy (*C* sites); and F-OH. Ordering may involve all of these pairs to varying degrees in an effort to achieve local charge-balance during crystal growth.

### Heating experiments

Attempts were made to disorder low vesuvianite from Eden Mills and Asbestos by heating portions of individual sectors extracted from larger crystals (Allen 1985). X-ray intensities of GVDs were measured for samples heated *in situ* to 500, 900, and 1,000°C, and for samples heated to 600, 700, 800, and 900°C for up to 50 days and then rapidly quenched. (Vesuvianite melts at approximately 1,100°C.) All attempts proved unsuccessful, as no significant changes in intensity were observed in any sample. Thus a disordering transformation either does not occur in these samples of vesuvianite or is simply too sluggish to detect on a laboratory time-scale. Interestingly, Allen & Buseck (1988)

were able to induce disorder by heating low-symmetry grossular from the Eden Mills assemblage.

The low-vesuvianite sample from Crestmore studied by Veblen & Wiechmann (1991) shows fine-scale twinning rather than growth sectors. Instead of forming an ordered structure during growth, this material appears to have undergone an ordering transformation from the high-symmetry form during slow cooling from high temperatures. Heating should reverse the ordering process, causing the twins to disappear as the material reverts back to the high-symmetry form. If a disordering transformation can be observed for this material, it suggests that fine-scale twinning may facilitate the mechanism of transformation. The difficulty of disordering low vesuvianite from Eden Mills and Asbestos may then be attributed to presence of relatively large ordered sectors rather than fine-scale twinning.

Naturally heated low vesuvianite may be found in regionally metamorphosed rodingites (metarodingites), *e.g.*, from the high-grade Leontine Alps (Evans *et al.* 1979) and in the Cascade Range (Frost 1975). It would be useful to know if samples of vesuvianite from these localities possess a low- or high-symmetry structure, determined simply by observing whether or not GVDs are present on precession photographs or in SAED. Presence of high symmetry would indicate that disordering takes place only at high temperatures over geological periods of time, such as during regional metamorphic events. On the other hand, were annealing to occur over long periods of time at elevated temperatures, the material might appear optically homogeneous (no growth sectors) but continue to exhibit low symmetry.

### CONCLUSIONS

We have shown that symmetry variations in vesuvianite can be attributed to differences in conditions of crystal growth. Models proposed within the past 20 years adequately account for the disordered structure of high-symmetry vesuvianite formed at relatively high temperatures and formed in contact deposits (skarns and hornfels) and regionally metamorphosed rocks (calc-schists). Cross-hatched twinning characteristic of high vesuvianite is probably a result of an ordering transformation upon cooling.

The problems encountered in some X-ray and TEM studies of low-symmetry vesuvianite are most likely a result of not being able to isolate suitable "single crystals". Specimens of low vesuvianite that grew metastably at low temperatures in hydrothermally altered rocks (rodingites, *etc.*) are comprised of ordered sectors or domains whose structures were determined by the two-dimensional

atomic arrangements exposed on the surfaces of growth steps. Macroscopically, low vesuvianite crystals appear "gemmy" and tend to be large and euhedral, with morphologies consistent with tetragonal symmetry. Looks are deceiving, however, because microscopically individual sectors exhibit lower-than-tetragonal symmetry, consistent with monoclinic or triclinic space-groups.

## ACKNOWLEDGEMENTS

We thank D.R. Veblen, R.G. Burns, J.B. Thompson, Jr., D.L. Bish, J.E. Post, and P.R. Buseck for many stimulating discussions about vesuvianite. R.E. Newnham kindly provided access to his SHG equipment. C.A. Francis and W.C. Metropolis of the Harvard Mineralogical Museum supplied us with wonderful samples, allowing us to appreciate fully the beauty of this mineral. We also thank F. Mazzi and an anonymous referee for their helpful reviews of the manuscript. This research was supported by NSF Grant EAR 79-20095 to CWB.

## REFERENCES

- AKIZUKI, M. (1984): Origin of optical variations in grossular - andradite garnet. *Am. Mineral.* **69**, 328-338.
- \_\_\_\_\_ (1987): An explanation of optical variation in yugawaralite. *Mineral. Mag.* **51**, 615-620.
- \_\_\_\_\_, HAMPAR, M.S. & ZUSSMAN, J. (1979): An explanation of anomalous optical properties of topaz. *Mineral. Mag.* **43**, 237-241.
- ALLEN, F.M. (1985): *Structural and Chemical Variations in Vesuvianite*. Ph.D. dissertation, Harvard Univ., Cambridge, Massachusetts.
- \_\_\_\_\_ & BURNHAM, C.W. (1983a): Structure refinement of an iron-poor vesuvianite. *Trans. Am. Geophys. Union* **64**, 353 (abstr.).
- \_\_\_\_\_ & \_\_\_\_\_ (1983b): Cation ordering in low-symmetry vesuvianite. *Geol. Soc. Am., Abstr. Program* **15**, 513.
- \_\_\_\_\_ & \_\_\_\_\_ (1985): Structural variations in vesuvianite: a comprehensive model. *Geol. Soc. Am., Abstr. Program* **17**, 511.
- \_\_\_\_\_ & BUSECK, P.R. (1988): XRD, FTIR, and TEM studies of optically anisotropic grossular garnets. *Am. Mineral.* **73**, 568-584.
- AREM, J.E. (1970): *Crystal Chemistry and Structure of Idocrase*. Ph.D. dissertation, Harvard Univ., Cambridge, Massachusetts.
- \_\_\_\_\_ (1973): Idocrase (vesuvianite) - a 250 year puzzle. *Mineral. Rec.* **4**, 164-174.
- \_\_\_\_\_ & BURNHAM, C.W. (1969): Structural variations in idocrase. *Am. Mineral.* **54**, 1546-1550.
- BUSING, W.R. (1981): WMIN, a computer program to model molecules and crystals in terms of potential energy functions. *Oak Ridge National Lab., Spec. Publ.* **5747**.
- CODA, A., DELLA GIUSTA, A., ISETTI, G. & MAZZI, F. (1970): On the crystal structure of vesuvianite. *Atti Accademia Scienze di Torino* **105**, 1-22.
- DEER, W.A., HOWIE, R.A. & ZUSSMAN, J. (1982): *Rock-Forming Minerals. 1A. Orthosilicates*. Longman, London.
- DOUGHERTY, J.P. & KURTZ, S.K. (1976): A second harmonic analyzer for the detection of non-centrosymmetry. *J. Appl. Cryst.* **9**, 145-158.
- EVANS, B.W., TROMMSDORFF, V. & RICHTER, W. (1979): Petrology of an eclogite-metarodingite suite at Cima di Gagnone, Ticino, Switzerland. *Am. Mineral.* **64**, 15-31.
- FITZGERALD, S., LEAVENS, P.B., RHEINGOLD, A.L. & NELEN, J.A. (1987): Crystal structure of a REE-bearing vesuvianite from San Benito County, California. *Am. Mineral.* **72**, 625-628.
- \_\_\_\_\_, RHEINGOLD, A.L. & LEAVENS, P.B. (1986a): Crystal structure of a Cu-bearing vesuvianite. *Am. Mineral.* **71**, 1011-1014.
- \_\_\_\_\_, \_\_\_\_\_ & \_\_\_\_\_ (1986b): Crystal structure of a non- $P4/nnc$  vesuvianite from Asbestos, Quebec. *Am. Mineral.* **71**, 1483-1488.
- FROST, B.R. (1975): Contact metamorphism of serpentinite, chloritic blackwall, and rodingite at Paddy-Go-Easy Pass, central Cascades, Washington. *J. Petrol.* **16**, 272-313.
- GIUSEPPETTI, G. & MAZZI, F. (1983): The crystal structure of a vesuvianite with  $P4/n$  symmetry. *Tschermaks Mineral. Petrog. Mitt.* **31**, 277-288.
- POST, J.E. & BURNHAM, C.W. (1986): Ionic modeling of mineral structures and energies in the electron gas approximation:  $TiO_2$  polymorphs, quartz, forsterite, diopside. *Am. Mineral.* **71**, 142-150.
- RUCKLIDGE, J.C., KOCMAN, V., WHITLOW, S.H. & GABE, E.J. (1975): The crystal structures of three Canadian vesuvianites. *Can. Mineral.* **13**, 15-21.
- TAKÉUCHI, Y., HAGA, N., UMIZU, S. & SATO, G. (1982): The derivative structure of silicate garnets in grandite. *Z. Kristallogr.* **158**, 53-99.
- THOMPSON, J.B., JR. (1981): Polytypism in complex

- crystals: contrasts between mica and classical polytypes. *In* Structure and Bonding in Crystals 2 (M. O'Keeffe & A. Navrotsky, eds.). Academic Press, New York (167-196).
- VALLEY, J.W., PEACOR, D.R., BOWMAN, J.R., ESSENE, E.J. & ALLARD, M.J. (1985): Crystal chemistry of a Mg-vesuvianite and implications of phase equilibria in the system CaO-MgO-Al<sub>2</sub>O<sub>3</sub>-SiO<sub>2</sub>-H<sub>2</sub>O-CO<sub>2</sub>. *J. Metamorph. Geol.* **3**, 137-153.
- WARREN, B.E. & MODELL, D.I. (1931): The structure of vesuvianite Ca<sub>10</sub>Al<sub>4</sub>(Mg,Fe)<sub>2</sub>Si<sub>9</sub>O<sub>34</sub>(OH)<sub>4</sub>. *Z. Kristallogr.* **78**, 422-432.
- YOSHIASA, A. & MATSUMOTO, T. (1986): The crystal structure of vesuvianite from Nakatatsu mine: reinvestigation of the cation site-populations and of the hydroxyl groups. *Mineral. J.* **13**, 1-12.
- VEBLER, D.R. & WIECHMANN, M.J. (1991): Domain structure of a low-symmetry vesuvianite from Crestmore, California. *Am. Mineral.* **76**, 397-404.
- Received February 14, 1991, revised manuscript accepted July 10, 1991.*